JOURNAL OF PROPULSION AND POWER
Vol. 13, No. 2, March–April 1997

# Counterflow Diffusion Flame of Methane and Methane/Hydrogen Mixed Fuel in Supersonic Flow

Kenichi Takita*
*Tohoku University, Aramaki, Sendai 980-77, Japan*
and
Takashi Niioka†
*Tohoku University, Katahira, Sendai 980-77, Japan*

**Counterflow diffusion flames of methane and methane/hydrogen mixed fuel, developed in the forward stagnation-flow region of a porous cylinder in supersonic flow, are analyzed numerically by solving the two-dimensional compressible Navier–Stokes equations for multispecies. In the case of methane single fuel, an appreciable strong reaction zone or a flame cannot be established in Mach 3 airflow for any air static temperature under 1100 K, and the maximum temperature coincides with the stagnation temperature of airflow. When hydrogen with high reactivity and high diffusivity is added to methane, a strong reaction zone clearly appears and the flame temperature increases more than the stagnation temperature of airflow because of the heat released by the chemical reaction. However, the flame temperature has a maximum around the mixing ratio of 20% hydrogen, and then the flame temperature and mole fractions of the reaction products for mixed fuel decreases with an increase of the mixing ratio of hydrogen.**

## Nomenclature

$c$ = sonic velocity
$\boldsymbol{E}$ = vectors of convective fluxes in $\xi$ direction
$\boldsymbol{Ev}$ = vectors of viscous fluxes in $\xi$ direction
$\boldsymbol{F}$ = vectors of convective fluxes in $\eta$ direction
$\boldsymbol{Fv}$ = vectors of viscous fluxes in $\eta$ direction
$J$ = Jacobian
$M$ = Mach number
$p$ = pressure
$\boldsymbol{Q}$ = vectors of conservation variables
$\boldsymbol{S}$ = vectors of source terms
$t$ = time
$U$ = contravariant velocity
$u$ = velocity in the $x$ direction
$v$ = velocity in the $y$ direction
$x$ = space coordinate
$y$ = space coordinate
$\eta$ = generalized curvilinear coordinate
$\xi$ = generalized curvilinear coordinate
$\rho_i$ = density of $i$ species

*Subscripts*
$i$ = species number
$j$ = grid number
$L$ = left-hand side of cell interface
$R$ = right-hand side of cell interface

## Introduction

AN understanding of the combustion mechanism in supersonic flow is needed for the development of the scramjet engine mounted on a space-plane or hypersonic transportation system. However, a strong coupling of chemical reaction and fluid dynamics, including shock waves, complicates the physics. Therefore, simplified models that involve essences of the phenomena, for instance, the supersonic reactive mixing layer,[1–4] have been investigated. Moreover, a counterflow diffusion flame, developed in the forward stagnation-flow region of a porous cylinder in supersonic airflow, has recently been analyzed by the authors as a case including effects of a shock wave, and they have also demonstrated the fundamental characteristics of the counterflow diffusion flame in supersonic flow for the first time.[5,6]

In the study of flames in supersonic flow, hydrogen has been assumed as a fuel of the scramjet engine. Although hydrogen is probably the most suitable fuel for the scramjet engine, the disadvantages posed by its low density and low boiling point have been pointed out. Therefore, research on methane as another possible fuel for the scramjet engine has been conducted.[7–9] However, a negative conclusion has been reached on the use of methane because of its low reactivity. For example, numerical simulations on ignition of methane in the supersonic mixing layer by Ju and Niioka[9] showed that the minimum temperature required of an airflow to attain ignition in the computational domain with a length of 16 cm was 2200 K. Enhancement of ignition and combustion characteristics of methane are thus required. One possibility that has been investigated is the addition of another fuel such as silane[10] or hydrogen.[9] An addition of hydrogen is considered a better choice because the on-board use of silane at the present stage entails many difficulties. If the reactivity of methane can be heightened by a small addition of hydrogen, methane will become a strong candidate for use as scramjet engine fuel.

Accordingly, the objective of the present study is to numerically calculate fundamental characteristics of the counterflow diffusion flame of methane and methane/hydrogen mixed fuel as a basic model for combustion in the scramjet engine, for example, a fuel injection normal to supersonic airstream. In particular, the flame stability limit for different Mach numbers and for different air static temperatures, considered as an important aspect in the design of the engine, is mainly investigated. In the case of hydrogen,[6] the increase of Mach number, yielding high pressure in the reference field, and consequently, resulting in a high reaction rate of hydrogen, broadens the flame stability limit. On the other hand, since a change of pressure has little effect on the flame stability limit of meth-

Received June 21, 1996; revision received Oct. 20, 1996; accepted for publication Oct. 28, 1996. 

*Research Associate, Department of Aeronautics and Space Engineering. E-mail: takita@cc.mech.tohoku.ac.jp. Member AIAA.

†Professor, Institute of Fluid Science. E-mail: niioka@ifs.tohoku.ac.jp.

ane,[11] the characteristics of methane flame may be different from those of hydrogen flame.

Moreover, from the microscopic viewpoint, the flow configuration in this paper will be connected to an elementary model of turbulent combustion in compressible flow-like combustion behind a shocklet.

## Formulation

The flowfield considered in this calculation is shown in Fig. 1. A supersonic main airflow coming from the infinite left-hand side and a fuel stream issued uniformly from a porous cylinder form a counterflow field behind a detached shock wave. The simulation is conducted using the two-dimensional compressible Navier–Stokes equations in the generalized curvilinear coordinate for multispecies. The equations are

$$\frac{\partial \boldsymbol{Q}}{\partial t} + \frac{\partial(\boldsymbol{E} - \boldsymbol{Ev})}{\partial \xi} + \frac{\partial(\boldsymbol{F} - \boldsymbol{Fv})}{\partial \eta} = \boldsymbol{S} \tag{1}$$

Only steady-state solutions are discussed in the following sections.

The data of specific heats and formation enthalpies for each species are given by JANAF tables.[12] The transport coefficients such as viscosity, thermal conductivity, and diffusion coefficients for the species are obtained by application of the kinetic theory,[13,14] based on the Chapman–Enskong's theory, and Wilke's mixing rule[15] is used for mixtures. The combustion model by Stahl and Warnatz,[16] as revised by Ju and Niioka,[9] is employed in the present study. The model was applied to counterflow geometry and given consideration in Refs. 9 and 16. Eighteen species [$O_2$, $H_2$, $H_2O$, H, $HO_2$, OH, O, $H_2O_2$, CO, $CO_2$, CH, $CH_2$, $CH_3$, $CH_4$, CHO, $CH_2O$, $C_2H_4$, and $N_2$(inert)] and 101 elementary reactions are included in the model.

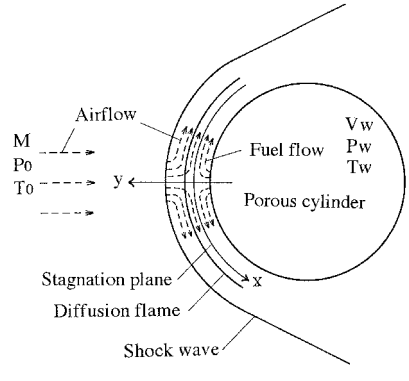


**Fig. 1 Schematic of the flow configuration.**

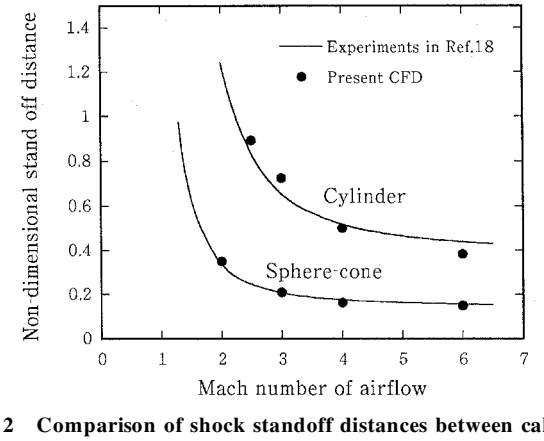


**Fig. 2 Comparison of shock standoff distances between calculation and experiments.**

The AUSM scheme[17–19] is used for the finite difference of convective terms to avoid a carbuncle phenomena that is numerically instable at a shock surface. It can be expressed in the generalized curvilinear coordinates as follows:

$$\boldsymbol{E}_{j+1/2} = \boldsymbol{E}^{(c)}_{j+1/2} + \boldsymbol{E}^{(p)}_{j+1/2}$$

$$= J\begin{bmatrix}\rho_1\\ \vdots\\ \rho_n\\ \rho u\\ \rho v\\ \rho H\end{bmatrix}_{j+1/2} U_{j+1/2} + J\begin{bmatrix}0\\ \vdots\\ 0\\ \xi_x p\\ \xi_y p\\ 0\end{bmatrix}_{j+1/2}$$

$$= J\sqrt{\xi_{kk}}\left\{\tfrac{1}{2}(M_\xi)_{j+1/2}\left[\begin{bmatrix}\rho_1 c\\ \vdots\\ \rho_n c\\ \rho c u\\ \rho c v\\ \rho H\end{bmatrix}_L + \begin{bmatrix}\rho_1 c\\ \vdots\\ \rho_n c\\ \rho c u\\ \rho c v\\ \rho H\end{bmatrix}_R\right]\right.$$

$$\left. - \tfrac{1}{2}\left|(M_\xi)_{j+1/2}\right|\Delta\begin{bmatrix}\rho_1 c\\ \vdots\\ \rho_n c\\ \rho c u\\ \rho c v\\ \rho H\end{bmatrix}\right\} + J\begin{bmatrix}0\\ \vdots\\ 0\\ \xi_x(p_L^+ + p_R^-)\\ \xi_y(p_L^+ + p_R^-)\\ 0\end{bmatrix}_{j+1/2} \tag{2}$$

where

$$H = (E + p)/\rho, \quad M_\xi = \frac{U_\xi}{c\sqrt{\xi_{kk}}}, \quad (M_\xi)_{j+1/2} = (M_\xi^+)_L + (M_\xi^-)_k$$

$$M_\xi^\pm = \begin{bmatrix}\pm\tfrac{1}{4}(M_\xi \pm 1)^2, & \text{if} \quad |M_\xi| \leqq 1\\ \tfrac{1}{2}(M_\xi \pm |M_\xi|), & \text{otherwise}\end{bmatrix}$$

$$p^\pm = \begin{bmatrix}(p/4)(M_\xi \pm 1)^2\cdot(2 \mp M_\xi), & \text{if} \quad |M_\xi| \leqq 1\\ (p/2)(M_\xi + |M_\xi|)/M_\xi, & \text{otherwise}\end{bmatrix}$$

$$\Delta[\cdot] = [\cdot]_R - [\cdot]_L$$

The numerical code is tested for the calculation of the nondimensional shock standoff distances of a cylinder and a sphere in supersonic flow. Figure 2 shows good agreement with the experimental data of Billig.[18]

Mach number $M$, static temperature $T_0$, and static pressure $P_0$ of the airflow, and velocity $V_w$ and temperature $T_w$ of the fuel flow are given as boundary conditions, and the diameter of the cylindrical porous burner is kept constant at 0.01 m. The numbers of $M$ and $T_0$ are chosen as the main parameters in the analysis to obtain fundamental characteristics of the counterflow diffusion flame in supersonic flow, as well as in the case of hydrogen single fuel.[6]

## Results and Discussion

### Effect of Air Static Temperature on Flames of Methane Single Fuel

The effect of air static temperature on the counterflow diffusion flame of methane single fuel is investigated first for constant conditions of Mach number ($M$ = 3.0) and pressure ($P_0$ = 0.01 MPa) in airflow, and of temperature ($T_w$ = 700 K) and velocity [$V_w$ = 100 m/s (Mach number is about 0.1)] in fuel flow. In conclusion, a strong reaction zone cannot be established in the Mach 3 airflow at any air $T_0$ under 1100 K,

although the stagnation temperature was higher than the ignition temperature (about 1600–2000 K) in the experiments by Bier et al.,[8] in which methane was injected into a hot airstream of Mach 2. This result is acceptable if considering a high stretch rate of the flowfield in Fig. 1 and a low stretch rate at extinction for methane flame that is much smaller than it is for hydrogen flame. In addition, the diffusion layer is much thinner than that of subsonic counterflow. Figure 3 shows the temperature distribution in the case of $T_0$ = 1100 K on the centerline of the cylindrical burner. The temperature jumps up to about 2500 K behind a detached shock wave, and increases gradually to a stagnation point. An increase of temperature around the stagnation point caused by heat released by the chemical reaction cannot be seen in Fig. 3. Furthermore, it is suggested that the very high concentration of O radical resolved from $O_2$ in airflow at such a high temperature has no effect on the establishment of the methane flame.

Figure 4 shows the maximum temperature for $M$ = 3.0 in terms of air static temperature. The maximum temperature increases linearly with air static temperature, coinciding with the air stagnation temperature. Figure 5 indicates the maximum mole fractions of $CO_2$ and $H_2O$ vs air static temperature. All products and radicals have the maximum concentration around a stagnation point where temperature and pressure become highest, as shown in the case of hydrogen.[6] Mole fractions of products and radicals increase with air static temperature; however, they are very small. For example, the maximum mole fraction of $H_2O$ is only 0.005, even when air static temperature becomes 1100 K and the stagnation temperature exceeds 2600 K. The increase in fractions of products on the log scale gradually weakens with an increase of air static temperature, as seen in Fig. 5. It is obvious from these results that an increase

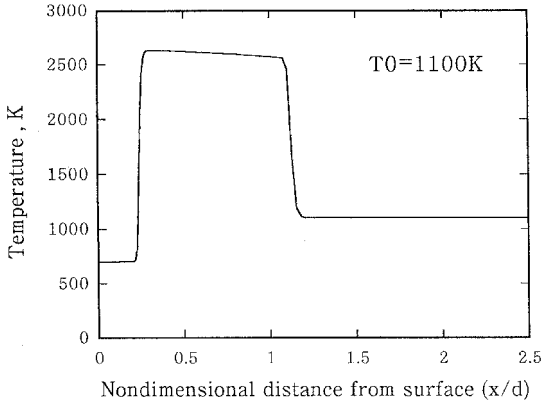


**Fig. 3 Temperature distribution on the centerline for $M$ = 3.0, $T_0$ = 1100 K, $V_w$ = 100 m/s, and $T_w$ = 700 K.**

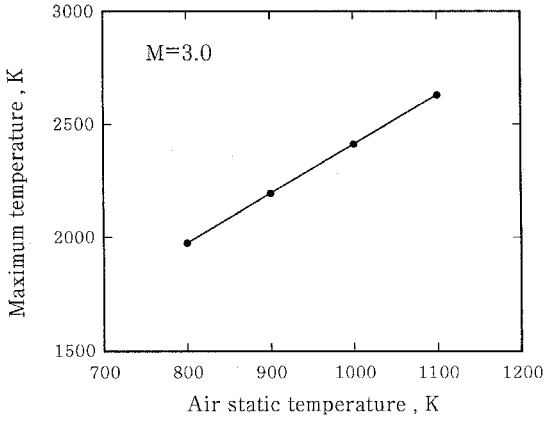


**Fig. 4 Dependence of the air static temperature on the maximum temperature for $M$ = 3.0.**

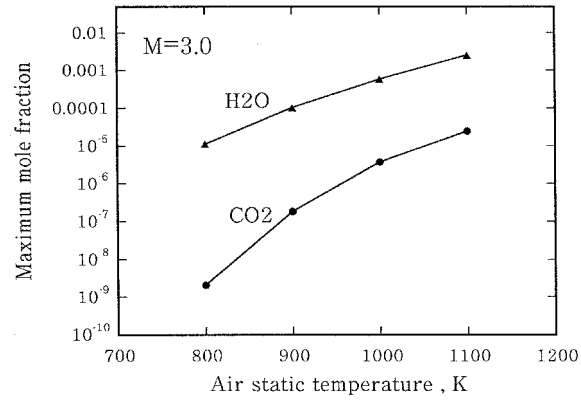


**Fig. 5 Dependence of the air static temperature on the maximum mole fractions of $H_2O$ and $CO_2$ for $M$ = 3.0.**

of air static temperature cannot form a strong reaction zone in the Mach 3 airflow.

Calculations are discontinued at $T_0$ = 1100 K, because above that point the stagnation temperature is more than 3000 K, making it impossible to estimate heat release by the chemical reaction, and results in more complicated problems, for example, the dissociation of $N_2$, which cannot be negligible.

### Effect of Mach Number on Flames of Methane Single Fuel

Temperature, pressure, and flow velocity in the shock-layer change with Mach number of the upstream airflow. Therefore, both positive and negative influences on the flame stability must be caused by a change of airflow Mach number and the flame mechanism must undergo major complicated changes. The flame stability for different flight Mach numbers is the most fundamental and interesting problem for the design of the scramjet engine.

The point at the left end in Fig. 4, whose boundary conditions are $T_0$ = 800 K, $P_0$ = 0.01 MPa, $T_w$ = 700 K, and $V_w$ = 100 m/s, is chosen first, to investigate the effect of change in Mach number in comparison with the change of air static temperature. Figure 6 shows the maximum temperature in terms of airflow Mach number, and Fig. 7 is the maximum mole fractions of $CO_2$ and $H_2O$. An increase of Mach number of airflow does not cause as strong a reaction in the stagnation-flow region as an increase of air static temperature, even though the range of Mach number is limited. The flame stability limit is independent of pressure for methane flame, in contrast to the case of hydrogen flame in which the stability limit proportionately increases with pressure, as reported by Balakrishnan et al.[11] Therefore, the positive effect of an increase of Mach number is only an increase of the stagnation temperature, and so it must result in the same effect as that of air static temperature. To form a strong reaction zone of methane single fuel, a decrease of airflow Mach number with high total temperature, which results in a large standoff distance of detached shock wave and a relaxation of high stretch rate, is desirable. However, it results in an extremely large computational domain that requires many mesh numbers and a very long computational time, because the stand-off distance of the detached shock wave increases nonlinearly at low Mach numbers.[5] This difficulty can also be simulated in the case of a cylindrical burner with a large diameter that has the same effect as a decrease of Mach number of airflow. Whether the counterflow diffusion flame of methane single fuel can be established in supersonic flow is a topic for future research.

### Effect of an Addition of Hydrogen to Methane

It is obvious from the previous discussion that the change of conditions on the air side is not so effective for the formation of a flame zone with a strong reaction. Moreover, our previous study on hydrogen[6] showed that conditions on the fuel side also had a weak impact on the flame stability limit,

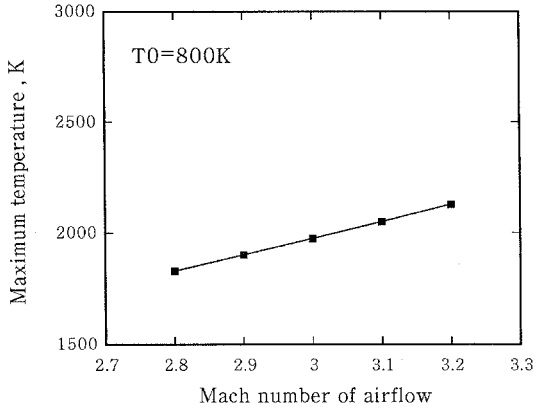


**Fig. 6 Dependence of the Mach number of the upper airflow on the maximum temperature in the reaction zone, for $T_0$ = 800 K and $V_w$ = 100 m/s.**

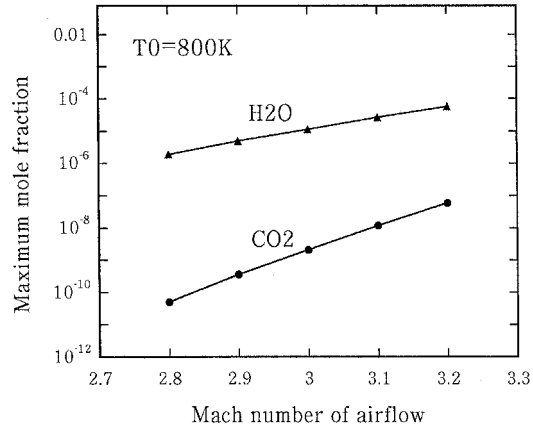


**Fig. 7 Dependence of the Mach number of airflow on the maximum mole fractions for $T_0$ = 800 K.**

except in the case of low-speed injection. Improvement in the reactivity of methane is an effective way to stabilize a flame in supersonic flow. Therefore, the effect of an addition of hydrogen to methane was investigated for constant airflow and fuel flow conditions, based on the assumption that the location of the shock wave and the stagnation plane does not change much with the mixing ratio, and therefore, does not affect combustion phenomena in the case of a small addition of hydrogen. Hydrogen has a much higher reactivity and higher diffusivity than methane, and so the addition of a small amount of hydrogen to methane may cause a strong reaction in the narrow mixing area.

When the volume ratio of hydrogen in methane/hydrogen mixed fuel becomes 20%, the maximum temperature abruptly increases about 100 K more than the stagnation temperature of airflow. The hydrogen fuel is a good source of H, OH, and O radicals. However, the consumption of H radicals by the reaction with methane molecules suppresses chain branching reactions at a low mixing ratio of hydrogen.[9] It can be considered that the ratio of H radicals becomes sufficient to maintain a strong reaction when the mixing ratio of hydrogen reaches 20%. Figure 8 is the temperature distribution at the centerline of the cylindrical body, clearly showing the heat release zone created from the chemical reaction. Detailed distributions of some products ($H_2O$, CO, $CH_3$, and O) at each grid point are plotted in Fig. 9 to show grid resolution, and differences of maximum point in each mole fractions can be recognized. Figure 10 shows the temperature contours around the cylindrical burner. This is the region where a strong reaction gradually disappears, as the distance from the centerline becomes larger. This is caused by a temperature decrease of airflow caused by thermal expansion and an increase of the flow stretch rate originating from the acceleration of the flow velocity along the flame sheet. The change of the flame temperature and mole fractions of species along the flame sheet is one of the typical characteristics of the counterflow diffusion flame in supersonic flow, as described in the case of hydrogen fuel.[6]

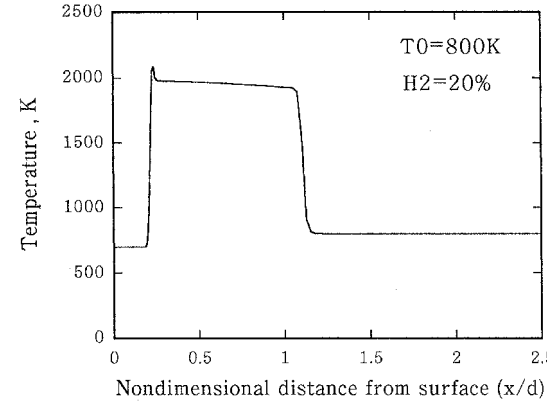


**Fig. 8 Temperature distribution on the centerline for $H_2$ 20%, $M$ = 3.0, and $T_0$ = 1100 K.**

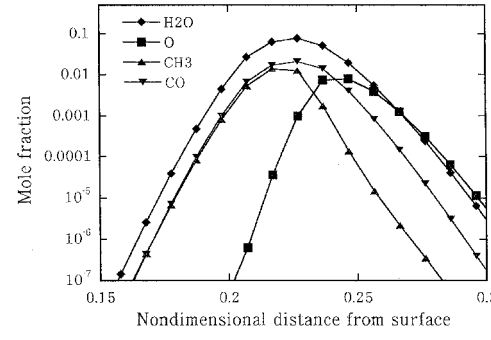


**Fig. 9 Mole fractions of products in reaction zone for the case of $H_2$ 20%.**

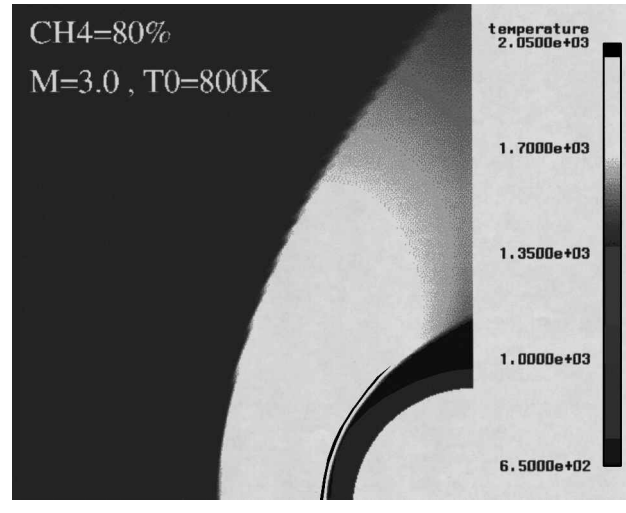


**Fig. 10 Temperature contour around the cylindrical burner for the case of $H_2$ 20%.**

Figure 11 shows the maximum mole fractions of $CO_2$ and $H_2O$ on the log scale vs the volume ratio of hydrogen in mixed fuel. These mole fractions increase rapidly with the volume ratio of hydrogen in contrast to the results shown in Figs. 5 and 7. It is revealed that the addition of hydrogen is much more effective for the formation of a strong reaction zone of methane fuel in the Mach 3 airflow than an increase of Mach number or airflow static temperature.

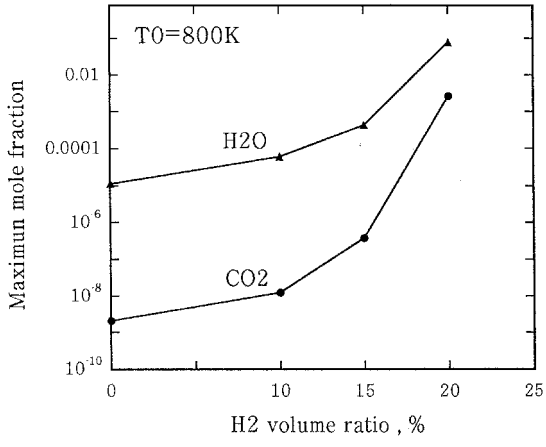


**Fig. 11 Effect of an addition of hydrogen to methane on the maximum mole fraction of $H_2O$ and $CO_2$, for $M$ = 3.0 and $T_0$ = 800 K.**

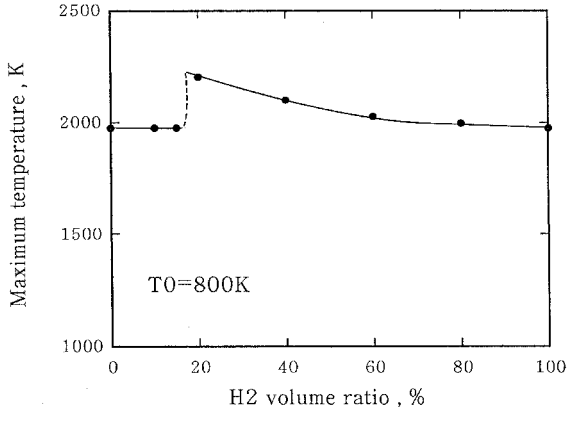


**Fig. 12 Dependence of the mixing ratio of mixed fuel on the maximum temperature for $M$ = 3.0 and $T_0$ = 800 K.**

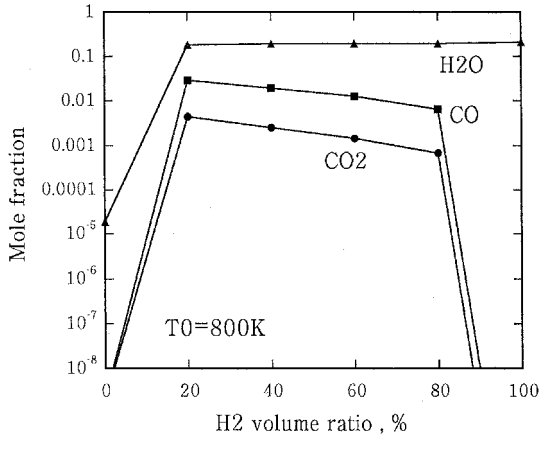


**Fig. 13 Dependence of the mixing ratio of mixed fuel on the mole fractions of $H_2O$, CO, and $CO_2$ for $M$ = 3.0 and $T_0$ = 800 K.**

### Overall Features of Methane/Hydrogen Mixed Fuel

Figure 12 shows the maximum temperature as a function of the mixing ratio of hydrogen in mixed fuel from 0 to 100%. In this figure, the mixing ratio was changed so that the momentum of fuel injection could be kept constant to maintain the same location of the shock wave and the stagnation plane; the stretch rate on the air side is also the same. The maximum temperature increases abruptly at 20% hydrogen. The reason is that no appreciable reaction zone can be established in Mach 3 airflow for a mixing ratio under 20%. The behavior of temperature around 20% is just as it is at ignition limit.

On the other hand, the flame temperature decreases with an increase of the mixing ratio of hydrogen in the range above 20%. This is a distinctive characteristic of the counterflow diffusion flame in supersonic flow, in contrast to the adiabatic temperature of premixed flame of hydrogen/methane mixed fuel, which increases monotonically with the mixing ratio of hydrogen. Furthermore, it is very interesting from a practical point of view, because it is generally expected that as the mixing ratio of hydrogen in mixed fuel becomes higher, the efficiency or the capacity of the engine increases. Some reasons for this result can be considered. When the momentum of fuel flow is constant, the fuel velocity increases with the ratio of hydrogen, and hydrogen has larger thermal conductivity than methane. Heat loss to fuel side by conduction and convection increases with the ratio of hydrogen in such a thin reaction zone very close to stagnation plane.

Figure 13 shows the maximum mole fractions of $H_2O$, CO, and $CO_2$ for each mixing ratio of mixed fuel. The mole fraction of CO is always higher than that of $CO_2$ because of high total temperature. The maximum values are obtained at 20% $H_2$, the same as the maximum temperature.

## Concluding Remarks

Counterflow diffusion flames of methane and methane/hydrogen mixed fuel in supersonic flow was numerically investigated. The summary of present results are shown as follows:

1) A strong reaction zone of methane single fuel cannot be established in the Mach 3 supersonic airflow at any air static temperature under 1100 K.

2) When hydrogen with a volume ratio exceeding 20% is added to methane, a strong reaction zone can be established and the temperature increases more than the stagnation temperature caused by the heat released by the chemical reaction. The maximum mole fraction of $CO_2$ and $H_2O$ increase rapidly with the mixing ratio of hydrogen, but only slightly with Mach number and static temperature of airflow.

3) The maximum flame temperature and the mole fractions of reaction products decrease with the mixing ratio of hydrogen above 20%.

## Acknowledgments

The authors thank Goro Masuya and Yiguang Ju of Tohoku University for their valuable suggestions. The first author is also grateful for the Japan Society for the Promotion of Science Fellowship for Japanese Junior Scientists.

## References

[1]Ju, Y., and Niioka, T., "An Asymptotic Analysis on Ignition with Chain-Branched Reaction in Supersonic Mixing Layer," *Archivum Combustion*, Vol. 11, 1991, pp. 151–168.

[2]Ju, Y., and Niioka, T., "Ignition Analysis of Unpremixed Reactants with Chain Mechanism in a Supersonic Mixing Layer," *AIAA Journal*, Vol. 31, 1993, pp. 863–868.

[3]Ju, Y., and Niioka, T., "Extinction of a Diffusion Flame in Supersonic Mixing Layer," *Combustion and Flame*, Vol. 97, 1994, pp. 423–428.

[4]Ju, Y., and Niioka, T., "Reduced Kinetic Mechanism of Ignition for Nonpremixed Hydrogen/Air in a Supersonic Mixing Layer," *Combustion and Flame*, Vol. 99, 1994, pp. 240–246.

[5]Takita, K., and Niioka, T., "Asymptotic Analysis on the Extinction of Diffusion Flames in Supersonic Stagnation-Point Flow," *JSME International Journal*, Vol. 39, 1996, pp. 440–445.

[6]Takita, K., and Niioka, T., "Numerical Simulation of Counterflow Diffusion Flame in Supersonic Airflow," *Proceedings of the 26th Symposium (International) on Combustion*, The Combustion Inst., Pittsburgh, PA, 1996 (to be published).

[7]Bier, K., Kappler, G., and Wilhelmi, H., "Experiments on the Combustion of Hydrogen and Methane Injected Transversely into an Supersonic Air Stream," *Proceedings of the 13th Symposium (International) on Combustion*, The Combustion Inst., Pittsburgh, PA, 1970, pp. 675–682.

[8]Bier, K., Kappler, G., and Wilhelmi, H., "Influence of the Injection Conditions on the Ignition of Methane and Hydrogen in a Hot Mach

2 Air Stream,'' *AIAA Journal*, Vol. 9, 1971, pp. 1865, 1866.
[9]Ju, Y., and Niioka, T., ''Ignition Simulation of Methane/Hydrogen Mixtures in a Supersonic Mixing Layer,'' *Combustion and Flame*, Vol. 102, 1995, pp. 462–470.
[10]Gerstein, M., and Choudhury, P. R., ''Use of Silane-Methane Mixtures for Scramjet Ignition,'' *Journal of Propulsion and Power*, Vol. 1, 1985, pp. 399–402.
[11]Balakrishnan, G., Smooke, M. D., and Williams, F. A., ''A Numerical Investigation of Extinction and Ignition Limits in Laminar Nonpremixed Counterflowing Hydrogen-Air Streams for Elementary and Reduced Chemistry,'' *Combustion and Flame*, Vol. 102, 1995, pp. 329–340.
[12]Chase, Jr., et al., ''JANAF Thermochemical Tables, 3rd ed.,'' *Journal of Physical and Chemical Reference Data*, Vol. 14, No. 1, 1985.
[13]Svehla, R. A., ''Estimated Viscosities and Thermal Conductivities of Gases at High Temperatures,'' NASA TR-132, 1962.
[14]White, F. M., ''Viscous Fluid Flow,'' McGraw–Hill, New York, 1974.
[15]Wilke, C. R., ''A Viscosity Equations for Gas Mixtures,'' *Journal of Chemical Physics*, Vol. 18, 1950, pp. 517–519.
[16]Stahl, G., and Warnatz, J., ''Numerical Investigation of Time-Dependent Properties and Extinction of Strained Methane- and Propane-Air Flamelets,'' *Combustion and Flame*, Vol. 85, 1991, pp. 285–299.
[17]Liou, M. S., and Steffen, C. J., ''A New Flux Splitting Scheme,'' *Journal of Computational Physics*, Vol. 107, 1993, pp. 23–39.
[18]Billig, F. S., ''Shock-Wave Shapes around Spherical- and Cylindrical-Nosed Bodies,'' *Journal of Spacecraft and Rockets*, Vol. 5, 1968, pp. 1247, 1248.
[19]Kano, S., Yamamoto, S., and Daiguji, H., ''An Efficient CFD Approach for Simulating Unsteady Hypersonic Shock-Shock Interference Flows,'' *Proceedings of the 6th International Symposium on Computational Fluid Dynamics*, Vol. 2, 1995, pp. 570–575.